

308

Scientific Notebook #247

Q200007170005



21
300

R

SHANNON COLTON

DAVID FERRILL

The Boorum & Pease® Quality Guarantee

The materials and craftsmanship that went into this product are of the finest quality. The pages are thread sewn, meaning they're bound to stay bound. The inks are moisture resistant and will not smear. And the uniform quality of the paper assures consistent rulings, excellent writing surface and erasability. If, at any time during normal use, this product does not perform to your expectations, we will replace it free of charge. Simply write to us:

Boorum & Pease Company
71 Clinton Road, Garden City, NY 11530
Attn: Marketing Services

Any correspondence should include the code number printed at the bottom of this page as well as the book title stamped at the bottom of the spine.

CNWRA
CONTROLLED
COPY 247

One Good Book Deserves Many Others.

Look for the complete line of Boorum & Pease® Columnar, Journal, and Record books. Custom-designed books also available by special order. For more information about our Customized Book Program, contact your office products dealer. See back cover for other books in this series.

Made in U.S.A.

Note: all files referenced here can be found on the USGS CD ROM or on the magnetic tape called ymflts.

Project: To build a 3D model of a Miocene tuff contact, the bottom of Tcr1, and faults at Yucca Mountain Nevada, concentrating on the Solitario Canyon Fault.

Purpose: To unravel the kinematic development of the fault.

Methods (Plan):

Step 1: Build a model of the the bottom of Tcr1, based on surface exposures of the contact.

- (a) Obtain surface UTM coordinates (X, Y) along the bottom of Tcr1 from USGS CD-ROM by Day et al. map
- (b) Obtain elevation values for X, Y coordinates
- (c) Convert data points to a format suitable for EarthVision
- (d) Build model on EarthVision

Step 2: Add faults as a simple model, in which the dips are constant along the fault's length.

- (a) Obtain surface UTM coordinates of Solitario Canyon Fault from USGS CD-ROM of Day et al. map
- (b) Obtain elevation values for X, Y coordinates
- (c) Convert data points to a format suitable for EarthVision
- (d) Build model on EarthVision

Step 3: Add available bed dip data where there are insufficient data points to determine bed dips from Tcr1 outcrops alone.

- (a) Obtain strike and dip data from USGS CD ROM
- <(b) Incorporate data into the model.

Step 4: Add available rake and plunge data to the model.

- (a) Obtain rake and plunge data along Solitario Canyon Fault from Simonds et. al. map at simons_view1.epr
- (b) Obtain additional rake and plunge data from USGS CD ROM
- <(c) Obtain points at depth of the Solitario Canyon Fault available through borehole data and cross section interpretations from CD ROM
- <(d) Incorporate data into the model.

Step 5: Consider the kinematic evolution of the fault. Build a model that fits with current thoughts about fault evolution (i.e. incorporate skills from journal articles)

- (a) Collect length and throw values along Solitario Canyon and neighboring faults from the 3D model
- (b) Plot length versus throw on Microsoft Excel Charts
- (c) Use throw profiles to evaluate fault behavior
- (d) modify model

1a. The CD ROM data was on the drive /bacr1, on BigBand. In accordit, the bottom of Tcr1 on the central block of Yucca

4 551031.35223 4082999.55434

NAD83, by conversion from state plane:

Tic ID	XTIC	YTIC
1	551057.23579	4075430.81524
2	545724.12198	4075412.01923
3	545896.89894	4083183.82520
4	551030.11225	4083202.45156

NAD83, with NADCON

Tic ID	XTIC	YTIC
1	550978.41185	4075424.75486
2	545845.08881	4075406.15328
3	545817.95801	4083177.82520
4	550951.30126	4083196.47096

Thus, we must find a method of converting NAD27 to NAD83 that will align the two maps properly before we sample the Z values.

The offset, and thus incorrect data values originally obtained were due to performing latticespot under the wrong NAD. The situation was corrected, and data points now look correct. A working hypothesis is that the USGS maps were actually in NAD83, rather than NAD27. Either the DEM was really NAD27 or the USGS map was really NAD83. I assumed the latter and the correct data points were collected.

Three arc coverages (located in the directory "arctoev") were converted to data points suitable to use in EarthVision. The key files include:

Arc files	Earthvision file	Description
FLTS	flts.dat	All faults on the 1:24000 digital map
MJFLTS	mjflts.dat	The major faults on the 1:24000 map, to be used in the model.
TCR1	tor1.dat	The horizon of the bottom of Tcr1.

Example of commands:

Conversion of FLTS to flts.dat:

Note: "Arc:" and "Generate" indicate that the command is performed in Arc, otherwise it is performed in an xterm.

```
Arc: precision double          *Sets precision to double precision
Arc: UNGENERATE LINE FLTS flts.lin  *uses coverage to create .lin file (ex: flts.lin)
Arc: quit                       *exits Arc
arc_line2arc_pts.nawk flts.lin > flts.pnt  *.nawk file uses .lin (ex: flts.lin) file with
                                         information on nodes of lines
                                         to create a .pnt file (ex: flts.pnt) with points
                                         at the node locations.

Arc: precision double          *Sets precision to double precision
Arc: Generate FLTS_PNT         *Turns .pnt file (ex: flts.pnt)
                               *into a coverage (ex: FLTS_PNT) with points

Generate: input flts.pnt
Generate: points
Generate: quit
Arc: PROJECT COVER FLTS_PNT FLTSPNT_U27 spcs27_2_utm27.prj *uses coverage projected in State Plane coordinates,
                                                           NAD27, zone 2702 (ex: coverage FLTS_PNT) to
                                                           create a coverage in
                                                           UTM NAD27, zone 11 (ex: coverage FLTSPNT_U27)
Arc: build FLTSPNT_U27 points  *builds point attribute table for coverage
```

```
Arc: LATTICESPOT ALL9UTM83 FLTSPNT_U27 z_elev
```

(ex: FLTSPNT_U27)
*collects elevation values by comparison with the DEM, ALL9UTM83, and places elevations in the point attribute table under the column z_elev for the coverage

```
Arc: ARCTIN FLTSPNT_U27 FLTS_TIN POINT z_elev
Arc: UNGENERATE TIN FLTS_TIN flts_xyz
```

*creates a TIN (ex: FLTS_TIN) with the coverage
*creates a .lin and .pnt (ex: flts_xyz.pnt) file from the tin.

```
Arc: quit
tinpnt2ev.nawk flts_xyz.pnt > flts.dat
```

*nawk code uses .pnt file to put X, Y, and Z coordinates of points in a format suitable for EarthVision.

- 1d. All EarthVision data was copied into a new file called ymev. It can be found on my home directory on the ONYX. A 2D grid was calculated for Tcr1, without any faults cutting it. Steps: Under Modeling/2-D Minimum Tension Gridding, scattered data was listed as tor1.dat. Calculate/Normal Minimum tension calculated the 2-D grid.
- 2a-c. Same procedure as 1a-c.
- 2d. Data was organized as follows:
The directory "ymev" contains data used in calculations of the 3D EarthVision models. The directory "origblks" contains the original fault data points, ("dat" files) and horizon points (tor1.dat) gathered from ArcInfo. The file "flts.dat" contains the data points for all faults on the 1:24000 map. The file "mjflts.dat" contains the data points for all faults currently included in the model, and the file "flts.ann" contains the names used in both origblks and slopespec for each fault. For example, "f1" indicates the Northern Windy Wash fault. The directory "slopespec" contains altered data points (for example, data points might be added north or south of the extent of the fault to constrain its location). The file tor1.dat was edited to remove data points very close to faults because they can mess up the calculation of block models. The edited version of tor1.dat is tor1edit.dat. It also includes 2D grids of each fault, 2D grid reports, sequence files (.seq) used in the Geologic Structure Builder, and faces files (.faces), which are the final models.

To see how each fault was added, see ymev/slopespec/howtoaddflt.txt
To see how the horizon Tcr1 was added, see howtoaddhorizon.txt
The final figures used in the thesis are in ymev/slopespec/thesisfigs.
Other images of the model at earlier stages are shown in slopespec/postscript, slopespec/rgb, and slopespec/showcase.

3a. Strike and dip data:

Arcedit was used to gather data on the strike and dip of beds. The data was available under the arc coverage BEDDIP. The coverage was displayed in an arcedit window. The draw environment was set to all features using "de all." Next to the window I placed a text file. The nodes did not have attributes, so I could not select them automatically to get X and Y coordinate data until I created attributes by using the arcedit commands "af node" and "createattributes." The arcedit command "af node" and "sel" allowed me to select a node at the center of the strike and dip symbol. Arcedit showed the X, Y coordinates (NAD27), and they were copied into the text file. To get each strike value, I would use the rotate function. However, nodes could not be

rotated, so I first added points at each node to the file with the arcdit commands "ef label" and "add," and saved the file with these labels. In each case, there were two labels, at the end of each strike line. I selected a label with "sel" (any label, it does not matter which is chosen), and used "rot" to rotate it the same angle from north that the strike makes. I selected from one end of the strike line then the other, choosing the order that would create the smallest angle out of 360 degrees. Arcdit tells you the rotation of that line counterclockwise from north. In order to get the accurate strike, i.e. clockwise from north instead of counterclockwise, the values were changed to 360-strike. The dips were printed next to the symbols, and simply typed into the text file.

Data on the strike and dip of beds is located in dipdat/beds.

4a. Rake and plunge data:

Universal Transverse Mercator coordinates, azimuth, and plunge data of fault dip vectors were obtained from "Map Showing Fault Activity in the Yucca Mountain Area, Nye County, Nevada" by Simonds et al., 1995. The data was gathered in the same manner as described for gathering the strike and dip data in 2a.

The data values are located in dipdat/fltplane.

The data was plotted for Northern Windy Wash, Fatigue Wash, Boomerang Point, Solitario Canyon, and Iron Ridge faults to look for consistent patterns along the length of faults.

Other than Northern Windy Wash, which steepens from north to south, there were not any patterns for the faults.

4b. Rake and plunge data was also gathered from the USGS CD ROM. The coverage used was FLTDP (located in arcfiles/unedited).

The fault dip data is located in dipdat/fltplane.

Slickenside data was also gathered from both maps (Simonds et al., 1995; Day et al., 1998). Data are located in dipdat/fltslick.

4c. Cross section data

Ron Martin did most of this for me.

We used DXFARC to extract arcs from the dxf image sitegeol. We then saved each line as a separate file in an arc coverage.

We located the beginning and ending points of the three cross section lines on the 1:24000 map by zooming in very close on arc coverages.

Ron wrote a shell script to collect points along the surface every 50m. It did not simply gather every 50m in the x direction, but a code was written to gather it based on the slope of the cross section line, so points are approximately every 50m on a string if you layed a string across the surface. We then went through a conversion process to get the Z values for each point and format the data for EarthVision. These data points are in state plane NAD 83.

They need to be converted to UTM NAD83 before they can be incorporated into the model. Data is located in xsevalueswrongNAD.

5a-b. A cumulative throw profile was drawn for the Solitario Canyon-Iron Ridge fault system.

7/14/00 - HLMSEK

The University of Texas at San Antonio

Three-Dimensional Model of a Faulted Miocene Tuff Layer at Yucca Mountain, Nevada

by
Shannon Lindsay Colton

An Honors Thesis

Submitted to the Faculty of the University Honors Program
in Partial Fulfillment of the Requirements

for

Graduation with University Honors Program Honors

Approved: Stuart Birnbaum May 27, 1998

Signature of Dr. Stuart J. Birnbaum Date

David A. Ferrill

Signature of Dr. David A. Ferrill

Eric R. Swanson

Signature of Dr. Eric R. Swanson

Spring 1998

HLM=K 7/19/00

Abstract--A three-dimensional model of five major faults, several smaller faults, and the contact between crystal-rich (Cr) and crystal-poor (Cp) Tiva Canyon Tuff was developed to reveal the geometry of fault blocks and unravel the kinematic development of major fault systems on western Yucca Mountain, Nevada. Geometry of fault blocks and net displacement along fault surfaces indicates that the western Yucca Mountain fault system is in an advanced state of fault development by segment linkage. Linkage has occurred by both curved tip propagation and connecting fault formation and has produced breached relay ramps. A cumulative throw profile reveals two local minima, where there are probably additional fault segments and/or deformation within relay ramps buried beneath Quaternary alluvium.

INTRODUCTION

Yucca Mountain is a faulted east-dipping cuesta in southwest Nevada composed of Miocene ash flow tuff layers. Yucca Mountain is in the western Basin and Range Province, an area with complex Miocene to present extensional and strike-slip faulting (Scott, 1990; Ferrill *et al.*, 1996; Morris *et al.*, 1996). The ridge capping layers at Yucca Mountain consist of various thermomechanical units of the Miocene Tiva Canyon Tuff (Day *et al.*, 1998). The faults at Yucca Mountain have been carefully mapped, however the relationships between major throughgoing faults and smaller faults or fault branches remains poorly constrained. Three-dimensional (3D) models of fault blocks in Yucca Mountain have been of relatively low resolution, limited by the number of faults included and data density on faulted horizons (Stirewalt *et al.*, 1994). The gross structural history of Yucca Mountain is fairly well known (Ferrill *et al.*, 1997; Stirewalt *et al.*,

HLM=K 7/19/00

Northern Windy Wash, Solitario Canyon, and Iron Ridge faults. Orientation data for the Northern Windy Wash fault displays an increase in fault dip to the south, but other faults do not show a pronounced increase or decrease to the south. Solitario Canyon and Iron Ridge fault dips vary widely within short distances (e.g. 25° in 200m). Due to the lack of data along some faults and the high variance of dip along other faults, the average dip for each fault was calculated, and each fault in the 3D model is portrayed with its average dip value along the entire length of the fault.

THREE-DIMENSIONSL MODEL DEVELOPMENT

A 3D model was developed to study the geometry of faults and fault blocks along western Yucca Mountain. The five major faults in the study area are the Northern Windy Wash, Fatigue Wash, Boomerang Point, Solitario Canyon, and Iron Ridge faults. The bottom of the Cr unit, a crystal-rich member of the Tiva Canyon Tuff, was the horizon selected from a 1:24,000 scale map of Yucca Mountain as the horizon with maximum outcrop exposure data to constrain the 3D horizon model (Day *et al.*, 1998). The map was available in digital format as a "dxf" file, indicating its origin as an AutoCad file. With ArcInfo version 7.0.2 software, the "dxf" file was converted to coverages containing the coordinates of fault dips, faults, and structural contour lines, all projected in State Plane coordinates, NAD83.

ArcEdit version 7.0.2 was used to delete from coverages all structural contour arcs except the bottom of Cr, and all faults except the five major faults listed above. The data would ultimately be modeled with EarthVision version 4.0.3 software, in which acceptable input

HLM:K 7/14/00

4

includes lines with a constant elevation and points. Points along each Cr-Cp contact varied in elevation. Thus, individual data points with unique elevations were necessary for the EarthVision model. Arcs were converted to sets of data points sampled along each arc. Elevations for each data point along arcs were sampled from a digital elevation map (DEM) of Yucca Mountain, with map coordinates and elevations sampled on a 30 meter grid. The DEM was projected in UTM zone 11, NAD83. The structural contour, fault, and fault dip maps were converted to UTM zone 11, NAD83 with the "NADCON" command in ArcInfo. Then, the "LATTICESPOT" command in ArcInfo was used to calculate each point elevation by reference to the DEM. A nawk code (written by Ronald Martin, CNWRA) was used to convert the file to a format suitable for EarthVision.

In EarthVision, several specific data points and the overall morphology of the horizon were checked by visual comparison to the 1:24,000 scale map. Individual faults were stored in separate data files. Two-dimensional (2D) grids were drawn for each fault. The grids accurately fit the data points for the fault; however control points were necessary to constrain the fault location at depth and height above the surface. To constrain 3D fault geometry, a nawk code was written to extrapolate each fault data point both up and down the fault surface based on the strike and dip of each fault. For each fault, this was performed to heights of 200m and 1000m, and to a depth of 1000m from the original data. The data at these three locations were concatenated to the original data, and the points were connected by 2D gridding. Since 2D grids cover the entire range of the model, EarthVision's Graphic Editor was used to draw clipping polygons which specified the range of faults to be used in further calculations, such as horizon gridding. For example, the Boomerang Point fault is contained in approximately the middle third

HLM:K 7/14/00

5

(from north to south) of the model. Some faults extend beyond the range of the model. For example, the Iron Ridge fault continues south of the model. In this case, a clipping polygon was drawn for the fault to continue north until it no longer appears at the surface, and terminate at some distance south of the model. EarthVision Geologic Structure Builder was used to establish a fault tree hierarchy, in which faulting order was specified. For example, Iron Ridge fault was set to terminate at the intersection of Iron Ridge and Solitario Canyon faults. A 3D model was calculated as specified by the fault tree hierarchy.

The contact between Cr and Cp was then edited and added to the model. Horizon data points along fault surfaces were removed as required in EarthVision to ensure calculation of a reasonable plane. Points along fault surfaces, if not removed, might be used within the wrong block during calculations and the resulting horizon can make steep, unsuitable curves to connect those points. Information about the horizon was added in the Geologic Structure Builder, and a horizon was calculated to fit the data points within the 3D fault structure previously built.

Distinct curves in the horizon surface remained at this point. For example, the data points between Solitario Canyon fault and Iron Ridge fault had several relatively abrupt decreases in elevation, indicative of fault offset. Faults in these locations were also mapped by Day *et al.* (1998) on the 1:24,000 scale geologic map. The largest of these faults was gathered from the converted Arc coverage by Day *et al.* (1998) and converted to EarthVision data points. No dip values were available for this fault. Other faults oriented in the same direction (NW) commonly have dips of 80 degrees. Thus, an 80 degree dip was applied to this fault. Another major flaw in the horizon was due to a complex system of faults between Northern Windy Wash and Fatigue Wash faults. Although there are many faults in that area, no single one was isolated

HLM=K 7/19/00

6

for the model. Instead, a connecting fault was modeled in the approximate area of the faults, and it was added to the model with a constant dip of 80 degrees. The resulting fault model showed connections between major faults (Fig. 2). The horizon was regrided, and revealed the largest undulations in the horizon surface had been removed by the addition of these faults (Fig. 3). There are several less pronounced steps remaining in the fault surface. For example, there are indications of faults in two areas north of Boomerang Point fault. These correspond in position to clusters of faults north of Boomerang Point fault on the 1:24,000 scale geologic map by Simonds *et al.* (1995).

FAULT GROWTH BY SEGMENT LINKAGE

During the last decade, there have been major advances in the understanding of the evolution and interaction of normal faults and fault systems (Childs *et al.*, 1997; Peacock and Sanderson, 1994; Trudgill and Cartwright, 1994) and scaling relationships for normal faults (Scholz *et al.*, 1993; Dawers and Anders, 1995; Dawers *et al.*, 1993). There are two end-member conceptual models of fault development. One is a single fault that grows larger as slip increases. The other is fault growth by segment linkage (Willemese *et al.*, 1995). Trudgill and Cartwright (1994) and Peacock and Sanderson (1994) describe the process of segment linkage, based on field work on faults varying from the meter scale to the kilometer scale. First, segments are unconnected and do not interact. The fault segments grow, and when interaction occurs near the tips, the segments are "soft-linked" by an area of complex deformation, such as a relay ramp. A relay ramp is the volume of rock between two overlapping fault segments that show



HLM=K 7/19/00

7

displacement transfer (Childs *et al.*, 1995). The relay ramp area experiences rotation (tilting) about an axis nearly perpendicular to the fault planes. The rock is often tilted toward the hanging wall and fractured. Both overlapping and underlapping "soft-linked" faults tend to show the steepest displacement gradients off-centered, toward relay structures (Willemese, 1997). As segment displacement continues, relay ramps develop faults. A "hard-linked" fault system exists when one or more connecting faults have developed between the original faults segments, or a fault tip curves until joining the other segment, directly transferring displacement between the two faults. Breakthrough by curved lateral propagation can leave only one relict fault tip in the area of overlap, whereas breakthrough by connecting fault formation can leave two relict fault tips. In both cases, relict relay ramps can remain on the hangingwall or footwall (Fig. 4) (Ferrill *et al.*, 1998).

Examples of segment linkage both by connecting fault formation and curved lateral propagation are present at Yucca Mountain. For example, the Northern Windy Wash and Fatigue Wash faults are joined by a complex system of connecting faults, and Iron Ridge joins Solitario Canyon by curved tip propagation (Ferrill *et al.*, 1998).

The Solitario Canyon fault can be divided into three segments separated by cusps: northern, middle, and southern segments. Where the segments join, the westward triangular protrusions are referred to as a "cusps." We interpret that the Solitario Canyon northern segment and splay formed as a single fault, isolated from the middle segment. The northern tip of middle segment grew to connect with the northern segment and splay. Once the two faults were "hard-linked" and the relay ramp was breached, the splay probably became relatively inactive.

H.L. MEK 7/19/00

8

The Iron Ridge fault seems to be in an earlier stage of the same process. Displacement on the southern segment of Solitario Canyon fault might decline or cease as the Iron Ridge accumulates more displacement. Over time, Iron Ridge fault would develop a larger net displacement, while the southern segment of the Solitario Canyon fault would experience decreased faulting activity until only a inactive relict tip may exist. Aside from a relict tip, another noticeable feature is the cusp where the faults intersect.

Northern Windy Wash and Fatigue Wash faults are connected by a complex area of faulting, with an overall trend to the NW (Ferrill *et al.*, 1998). Although these two faults are now connected by a throughgoing connecting fault system, the fault linkage has apparently not led to segment abandonment on Northern Windy Wash fault. Mapping by Simonds *et al.* (1995) suggests that the segments of the Northern Windy Wash fault, both north and south of the connecting fault system, and the Fatigue Wash fault south of the connecting fault system, have been active in the late Quaternary. The northern part of the Fatigue Wash fault is interpreted by Simonds *et al.* (1995) to display no evidence of Quaternary displacement, consistent with an interpretation that formation of the current fault system has led to abandonment of the northern segment of the Fatigue Wash fault.

THROW VERSUS DISTANCE DIAGRAMS

Throw versus distance diagrams can be used to interpret fault interactions. Generally, faults may be unlinked, or linked by a branch point or a branch line (Childs *et al.*, 1997). Linked faults can be plotted on a throw versus distance diagram to study displacement patterns

H.L. MEK 7/19/00

9

for the fault system. For a linked fault system, the curves for each linked fault are added together to form a cumulative profile. The cumulative profile generally resembles the profile expected for one fault; maximum displacement occurs near the center, with zero displacement on the ends. The cumulative fault throw profile for a segmented fault system, however, is more complex than a single fault throw profile (Dawers and Anders, 1995). If deformations within relay ramps are not included in the cumulative profile, there are often, but not always, local minima of cumulative throw at relay ramp locations (Peacock and Sanderson, 1994).

Solitario Canyon and Iron Ridge faults were plotted on a distance-throw graph (Fig. 5). The Solitario Canyon fault shows local displacement minima where Iron Ridge fault joins Solitario Canyon fault, and south of this intersection where NW trending faults are present. These minima can be explained by deformation within the relay ramp between Solitario Canyon and Iron Ridge faults and displacement transfer to Iron Ridge Fault. Individual faults normally have a bow or C-shaped throw profile, with maximum displacement near the center and zero displacement at the ends. The Iron Ridge fault does not show zero displacement at its northern end. The Iron Ridge fault, however, is no longer isolated. Instead it is physically linked (hard-linked) to Solitario Canyon faults.

Fault throws on the model were added to form a cumulative throw profile. The cumulative throw profile has non-zero displacement at the southern end because faults continue beyond the model range to the north and south. Local throw minima at approximately 4.8km, 5.9km, and 7km correspond to the following fault (or segment) intersections, respectively: the northern and middle sections of the Solitario Canyon fault, the Solitario Canyon and the Iron Ridge faults, and the middle and southern sections of the Solitario Canyon fault.

ULLM EK 7/14/00

10

CONCLUSIONS

Other than Northern Windy Wash, which steepens from north to south, faults on western Yucca Mountain between UTM 544040 and 549000 do not show a correlation between dip angle and latitude. Large-scale fault-plane corrugations are evident on the Iron Ridge-Solitario Canyon fault system. Connecting faults are present between the Fatigue Wash and Northern Windy Wash faults. Connecting faults and curved tips trend NW (Ferrill *et al.*, 1998). The fault throw profile of Iron Ridge fault does not have a C-shape. It shows non-zero displacement at the northern end, where displacement is directly transferred to Solitario Canyon fault. Fault throw is high at cusps on Solitario Canyon and along connecting faults to the west, indicating an advanced state of fault interaction in which relay ramps have been breached.

Acknowledgements—I thank Ron Martin for sharing his technical computer expertise while training me for this project. I thank Darrell Sims for patiently teaching me concepts of fault scarp shapes and cumulative throw profiles, and for his good humor and encouragement. I thank David Ferrill, Stuart Birnbaum, and Eric Swanson for reviews which greatly improved the final paper, with special thanks to David Ferrill for sharing his extensive knowledge of structural geology and the geology of Yucca Mountain, for providing numerous articles about geologic studies of Yucca Mountain, and for his patient guidance throughout the project.

HLLM EK 7/14/00

11

REFERENCES

- Childs, C., Watterson, J. and Walsh, J.J. (1995) Fault overlap zones within developing normal fault systems. *Journal of the Geological Society, London* 152, 535-549.
- Dawers, N.H. and Anders, M.H. (1995) Displacement-length scaling and fault linkage. *Journal of Structural Geology* 17, 607-614.
- Dawers, N.H., Anders, M.H. and Scholz, C.H. (1993) Growth of normal faults: displacement-length scaling. *Geology* 21, 1107-1110.
- Day, W.C., Potter, C.J., Sweetkind, D.S., Dickerson, R.P., and San Juan, C.A., (1997) Bedrock Geologic Map of the Central Block Area, Yucca Mountain, Nye County, Nevada. U.S. Geological Survey Miscellaneous Investigations Investigation Series Map I-6201. Scale 1:6,000. U.S. Geological Survey, Denver, CO.
- Day, W.C., Dickerson, R.P., Potter, C.J., Sweetkind, D.S., San Juan, C.A., Drake, R.M. II and Fridrich, C.J. (1998) Geologic Map of the Yucca Mountain Area, Nye County, Nevada, Draft. Scale 1:24,000. U.S. Geological Survey: Denver, CO.
- Ferrill, D.A., Stirewalt, G.L., Henderson, D.B., Stamatakos, J.A. Morris, A.P., Wernicke, B.P., and Spivey, K.H. (1996) *Faulting in the Yucca Mountain Region: Critical Review and Analysis of Tectonic Data from the Central Basin and Range*. NUREG/CR-6401. U.S. Nuclear Regulatory Commission, Washington D.C..
- Ferrill, D.A., Connor, C.B., Stamatakos, J.A., Mckague, H.L., Hill, B.E., Ofoegbu, G.I. and Terhune, R. (1997) *Modeling fault-dike interaction: implications for lateral diversion of dikes and alignment of volcanoes in the Yucca Mountain (Nevada)*

HLM=K 7/19/00

12

- Region. CNWRA Intermediate Milestone 20-5708-471-760. Center for Nuclear Waste Regulatory Analyses: San Antonio, TX.
- Ferrill, D.A., Stamatakos, J.A. and Sims, D., in press, Normal Fault Corrugation: Implications for Growth and Seismicity of Active Normal Faults. Submitted to *Journal of Structural Geology*.
- Morris, A.P., Ferrill, D.A., and Henderson, D.B. (1996) Slip tendency analysis and fault reactivation. *Geology* **24**, 275-278.
- Peacock, D.C. and Sanderson, D.J. (1994) Geometry and development of relay ramps in normal fault systems. *American Association of Petroleum Geology Bulletin* **78**, 147-165.
- Sawyer, D.A., Fleck R.J., Lanphere, M.A., Warren, R.G., Broxton, D.E. and Hudson, M.R. (1994) Episodic caldera volcanism in the Miocene southwestern Nevada volcanic field: revised stratigraphic framework, $^{40}\text{Ar}/^{39}\text{Ar}$ geochronology, and implications for magmatism and extension. *Geological Society of America Bulletin* **106**, 1304-1318.
- Scholz, C.H., Dawers, N.H., Yu, J.-Z. and Anders, M.H. (1993) Fault growth and fault scaling laws: preliminary results. *Journal of Geophysical Research* **98**, 21,951-21,961.
- Scott, R.B. (1990) Tectonic setting of Yucca Mountain, southwest Nevada, in Wernicke, B.P. (ed.), Basin and Range Extensional Tectonics near the Latitude of Las Vegas, Nevada: Boulder, Colorado. *Geological Society of America Memoir* **176**, p. 251-282.
- Simonds, W.F., Whitney, J.W., Fox, K., Ramelli, A., Yount, J.C., Carr, C.D., Menges, R., Dickerson, R. and Scott, R.B. (1995) Map of Fault Activity of the Yucca Mountain Area, Nye County, Nevada. U.S. Geological Survey Miscellaneous Investigations Series, Map

HLM=K 7/19/00

13

- I-2520. Scale 1:24,000.
- Stirewalt, G.L., Young, S.R. and Henderson, D.B. (1994) A Preliminary Three-Dimensional Model for Yucca Mountain, Nevada: Report to Accompany Model Transfer to the Nuclear Regulatory Commission. CNWRA 94-023. Center for Nuclear Waste Regulatory Analyses, San Antonio, TX.
- Trudgill, B., and Cartwright, J. (1994) Relay-ramp forms and normal-fault linkages, Canyonlands National Park, Utah. *Geological Society of America Bulletin* **106**, 1143-1157.
- Willemsse, E.J. (1997) Segmented normal faults: correspondence between three-dimensional mechanical models and field data. *Journal of Geophysical Research* **102**, 675-692.
- Willemsse, E.J., Pollard, D.D., and Aydin, A. (1996) Three-dimensional analyses of slip distributions on normal fault arrays with consequences for fault scaling. *Journal of Structural Geology* **18**, 295-309.

HLM:K 7/14/00

14

FIGURE CAPTIONS

Table 1. Fault orientation data for Northern Windy Wash, Fatigue Wash, Boomerang Point, Solitario Canyon, Iron Ridge faults, compiled from maps by Simonds *et al.* (1995) and Day *et al.* (1998). Coordinates are in UTM zone 11, NAD83.

Fig 1. Fault dip versus latitude for (a) Northern Windy Wash, (b) Fatigue Wash, (c) Boomerang Point, (d) Solitario Canyon, and (e) Iron Ridge faults. Orientation data for the Northern Windy Wash fault show an increase in fault dip to the south, whereas orientation data for Fatigue Wash, Boomerang Point, Solitario Canyon, and Iron Ridge faults show no pronounced along-strike trend.

Fig 2. Three-dimensional model of major faults of western Yucca Mountain. The five major N-S faults are, from west to east, Northern Windy Wash, Fatigue Wash, Boomerang Point, Solitario Canyon, and Iron Ridge faults. Only the west-dipping portion of Solitario Canyon Fault is included. Fault dips are the average dips shown in Table 1. Also shown with 80 degree dips are a fault between Northern Windy Wash and Fatigue Wash faults, and a fault within the relay ramp between Iron Ridge and Solitario Canyon faults. Coordinates labeled on the model are in meters. Long horizontal dimension of model = 14900m, short horizontal dimension of model = 4954m, vertical dimension of model = 1340m.

Fig. 3. (a) White points indicate data points used to build the 3D model of the bottom of Cr in the Miocene Tiva Canyon Tuff. At each point, the bottom of Cr, a crystal-rich member of the Tiva



HLM:K 7/14/00

15

Canyon Tuff is exposed at the Earth's surface. (b) Three-dimensional model of major faults shown in Figure 2 and the horizon defined by the bottom of Cr. Block dimensions are the same as in Figure 2.

Figure 4. Evolution of fault growth and relay ramp development. (a) Breakthrough of an echelon array by curved lateral propagation causes large scale corrugations. Relict fault tips are depicted on the hangingwall. Only one relict fault tip occurs in the area of fault overlap. (b) Breakthrough by connecting fault formation eventually leads to individual segments with large centers and small relict tips. Connecting faults are often nearly as large as segments. Here, two relict fault tips occur per area of fault overlap. Fault tips are shown in both the hangingwall and the footwall. From Ferrill *et al.*, 1998.

Figure 5. Yucca Mountain distance versus throw profiles. Solitario Canyon fault is the heavy solid line, and Iron Ridge fault is the light solid line. The cumulative throw profile (dashed line) is the sum of throws of Solitario Canyon and Iron Ridge faults. Local throw minima at approximately 4.8km, 5.9km, and 7km correspond to the following fault (or segment) intersections, respectively: the northern and middle sections of the Solitario Canyon fault, the Solitario Canyon and Iron Ridge faults, and the middle and southern sections of the Solitario Canyon fault.

HLMCK 7/19/00

Data Source	UTM Coordinates	Strike	Dip	Data Source	UTM Coordinates	Strike	Dip
Northern Windy Wash				Solitario Canyon (continued)			
Day et. al	545139.53	4083696	309 46	Day et. al	546614.02	4073868.3	355 69
Day et. al	545107.71	4082908.7	1 55	Day et. al	546612.11	4073834.5	354 66
Day et. al	545121.31	4082718.2	353 55	Day et. al	546585.65	4073254.2	354 48
Day et. al	545033.64	4082103.6	5 64	Day et. al	546580.22	4073026.3	360 62
Day et. al	544948.63	4081652	25 65	Day et. al	546544.58	4072851.8	4 75
Day et. al	544936.41	4081580.6	329 78	Day et. al	546409.5	4072160.6	4 55
Day et. al	544927.8	4081114.6	320 80	Simonds et. al	546182.82	4071367.5	360 81
Day et. al	545034.51	4080953.5	350 80	Simonds et. al	546249.72	4071594.8	63 80
		Dip average 65		Simonds et. al	546276.33	4071705.8	352 52
				Simonds et. al	546319.67	4071760.6	1 85
Fatigue Wash Fault				Simonds et. al	546318.59	4071761.5	5 85
				Simonds et. al	546349.59	4071848.3	5 60
Day et. al	545020.01	4078247.3	1 72	Simonds et. al	546360.81	4071915.3	4 60
Day et. al	544841.89	4077672	359 70	Simonds et. al	546367.31	4072005.3	357 66
Day et. al	544756.53	4077365.7	359 80	Simonds et. al	546222.65	4071939.2	8 76
		Dip average 74		Simonds et. al	546480.46	4072697.4	27 68
				Simonds et. al	546497.34	4072793.4	3 72
Boomerang Point Fault				Simonds et. al	546528.99	4072939	21 70
Day et. al	545942.68	4078040.6	218 85	Simonds et. al	546554.31	4073019.2	24 70
		Dip average 85		Simonds et. al	546571.18	4073121.5	358 58
				Simonds et. al	546582.79	4073461.2	347 80
Solitario Canyon				Simonds et. al	546602.4	4073646.1	333 56
Day et. al	547411.83	4080386	13 85	Simonds et. al	546611	4073791.8	360 69
Day et. al	547452.23	4079346.3	8 75	Simonds et. al	546610.09	4073842.5	29 72
Day et. al	547407.46	4079222.3	15 70	Simonds et. al	546597.88	4073923	339 61
Day et. al	547299.3	4078357.7	358 80	Simonds et. al	546839.55	4074441.6	7 60
Day et. al	547349.08	4077985.8	23 70	Simonds et. al	547002.44	4074685.8	34 68
Day et. al	547272.21	4077905	1 75	Simonds et. al	547050.38	4074781.3	23 60
Day et. al	547267.56	4077815.5	356 80	Simonds et. al	547078.1	4074831.9	27 60
Day et. al	546920.59	4076914.8	7 80	Simonds et. al	547098.57	4074926.2	6 80
Day et. al	546888.44	4076841.2	6 65	Simonds et. al	547067.42	4075318.9	348 70
Day et. al	546876.94	4076813.7	2 76	Simonds et. al	547067.39	4075318.9	348 65
Day et. al	546843.15	4076738.2	8 80	Simonds et. al	547001.74	4075775.2	4 57
Day et. al	546887.93	4076340.4	331 55	Simonds et. al	547011.25	4075978.1	9 54
Day et. al	547018.29	4075887.2	2 66	Simonds et. al	547016.73	4076011.8	7 53
Day et. al	547021.93	4075769.5	15 56	Simonds et. al	546951.68	4076073.6	325 75
Day et. al	547017.62	4076117.3	301 52	Simonds et. al	547021.52	4076130.5	344 48
Day et. al	547029.88	4076008.5	8 48	Simonds et. al	547004.73	4076175.9	330 52
Day et. al	547055.79	4075352	341 73	Simonds et. al	546855.24	4076444.5	352 55
Day et. al	547077.98	4075301.8	339 65	Simonds et. al	546839.41	4076541.5	2 61

Table 1

HLMCK 7/19/00

Data Source	UTM Coordinates	Strike	Dip	Data Source	UTM Coordinates	Strike	Dip
Solitario Canyon (continued)				Iron Ridge			
Simonds et. al	546855.41	4076663.5	81 70	Day et. al	547674.73	4073145.3	359 65
Simonds et. al	546834.25	4076798.5	34 80	Simonds et. al	547779.61	4071683	351 58
Simonds et. al	546871.38	4076882.1	21 85	Simonds et. al	547808.25	4071495.6	15 70
Simonds et. al	547125.15	4077241.3	28 75	Simonds et. al	547781.36	4071299.7	23 72
Simonds et. al	547125.69	4077241.2	28 75	Simonds et. al	547792.25	4070958.2	16 84
Simonds et. al	547142.48	4077468.8	338 80	Simonds et. al	547800.9	4070867.6	311 55
Simonds et. al	547180.63	4077616.8	359 70	Simonds et. al	547796.4	4070355.9	3 80
Simonds et. al	547228.75	4077809.8	9 80	Simonds et. al	547777.75	4070210.8	357 70
Simonds et. al	547236.57	4077832.4	31 75	Simonds et. al	547770.2	4070096.7	20 75
Simonds et. al	547247.4	4077878.9	353 75	Simonds et. al	547728.7	4069809.7	7 75
Simonds et. al	547287.95	4078353.5	13 80	Simonds et. al	547709	4069658.5	10 60
Simonds et. al	547402.71	4080381.7	9 85	Simonds et. al	547655.79	4069432.5	4 65
Simonds et. al	547436	4080570	13 60	Simonds et. al	547606.16	4069191.8	4 73
Simonds et. al	547445.06	4080629.3	360 60	Simonds et. al	547543.8	4068921.4	18 80
Simonds et. al	547468.01	4080749.5	3 65	Simonds et. al	547497.3	4068773.6	35 80
Simonds et. al	547559.3	4081445.3	28 86	Simonds et. al	547510.31	4068568.5	4 65
Simonds et. al	547680.1	4082965.5	358 80	Simonds et. al	547536.93	4068466.6	339 75
Simonds et. al	547676.07	4083182.5	356 85	Simonds et. al	547535.9	4068291.6	344 75
		Dip average 76		Simonds et. al	547702.64	4067953.1	119 70
				Simonds et. al	547733.98	4067975.5	341 70
				Simonds et. al	547796.06	4067851.2	136 60
				Simonds et. al	547893.7	4067730.1	338 60
				Simonds et. al	548011.69	4067283.1	315 65
						Dip average 70	

Table 1 (continued)

HLM EK 7/14/00

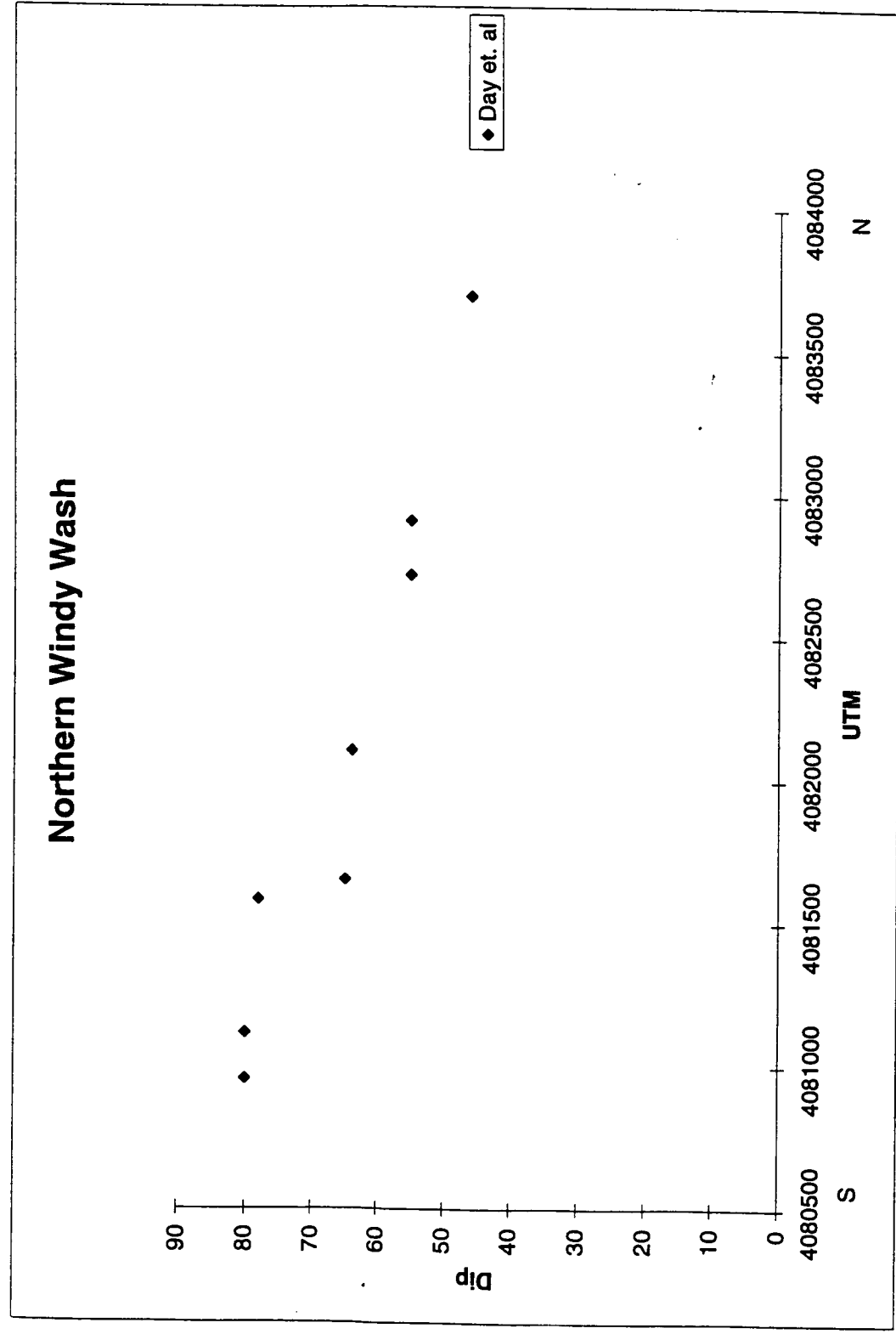
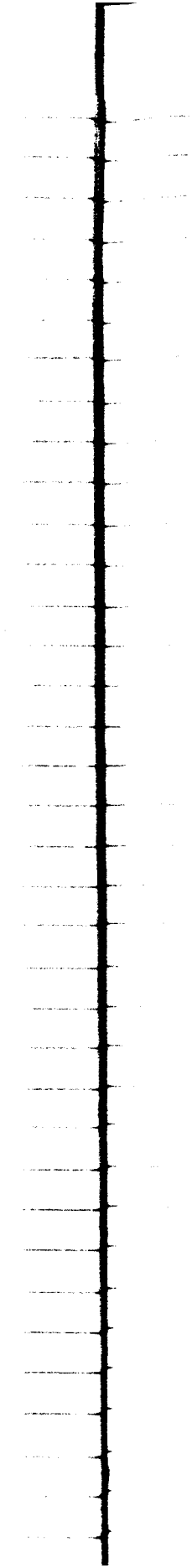


Figure 1a.



HLM EK 7/14/00

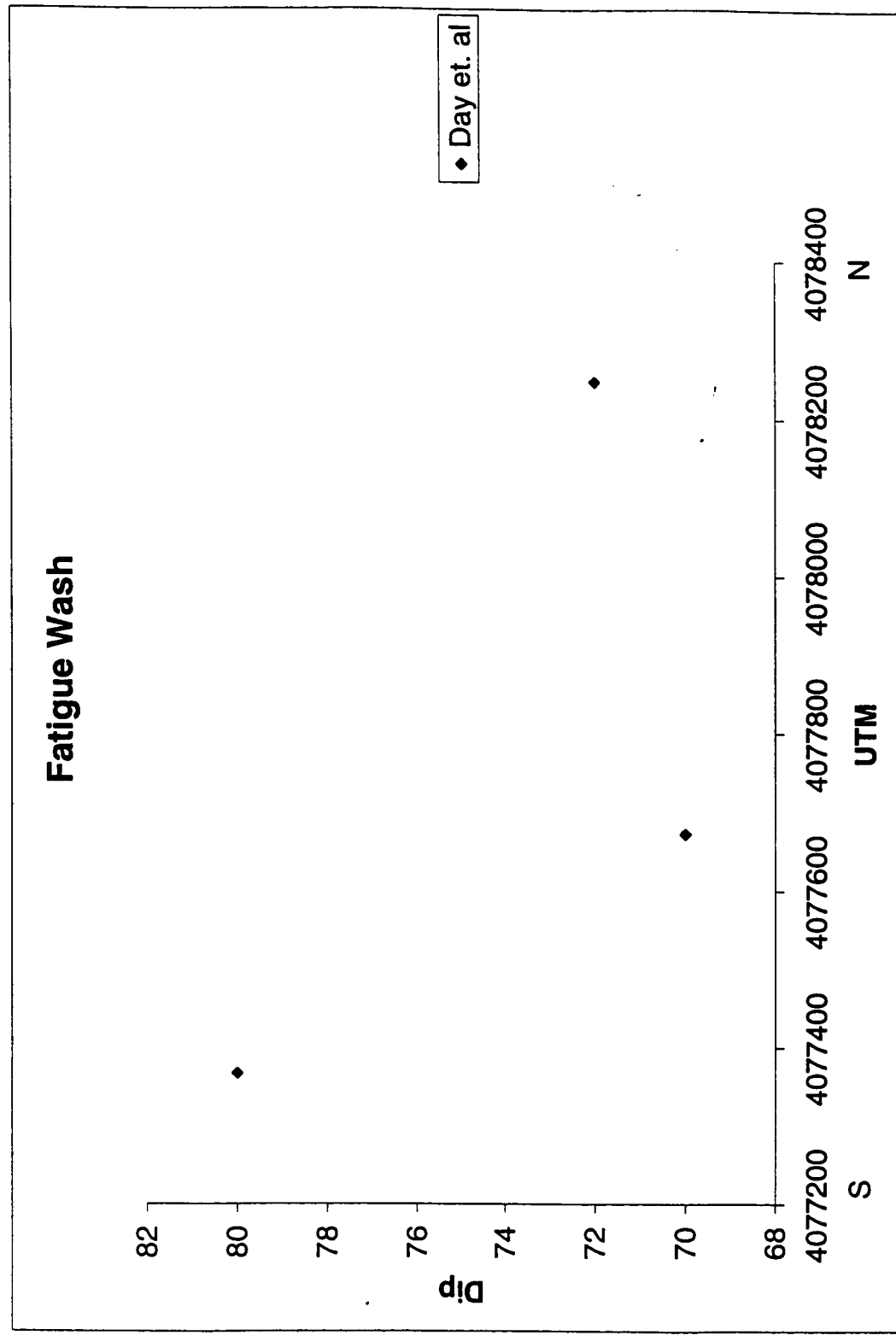


Figure 1b.

HLMCK 7/19/00

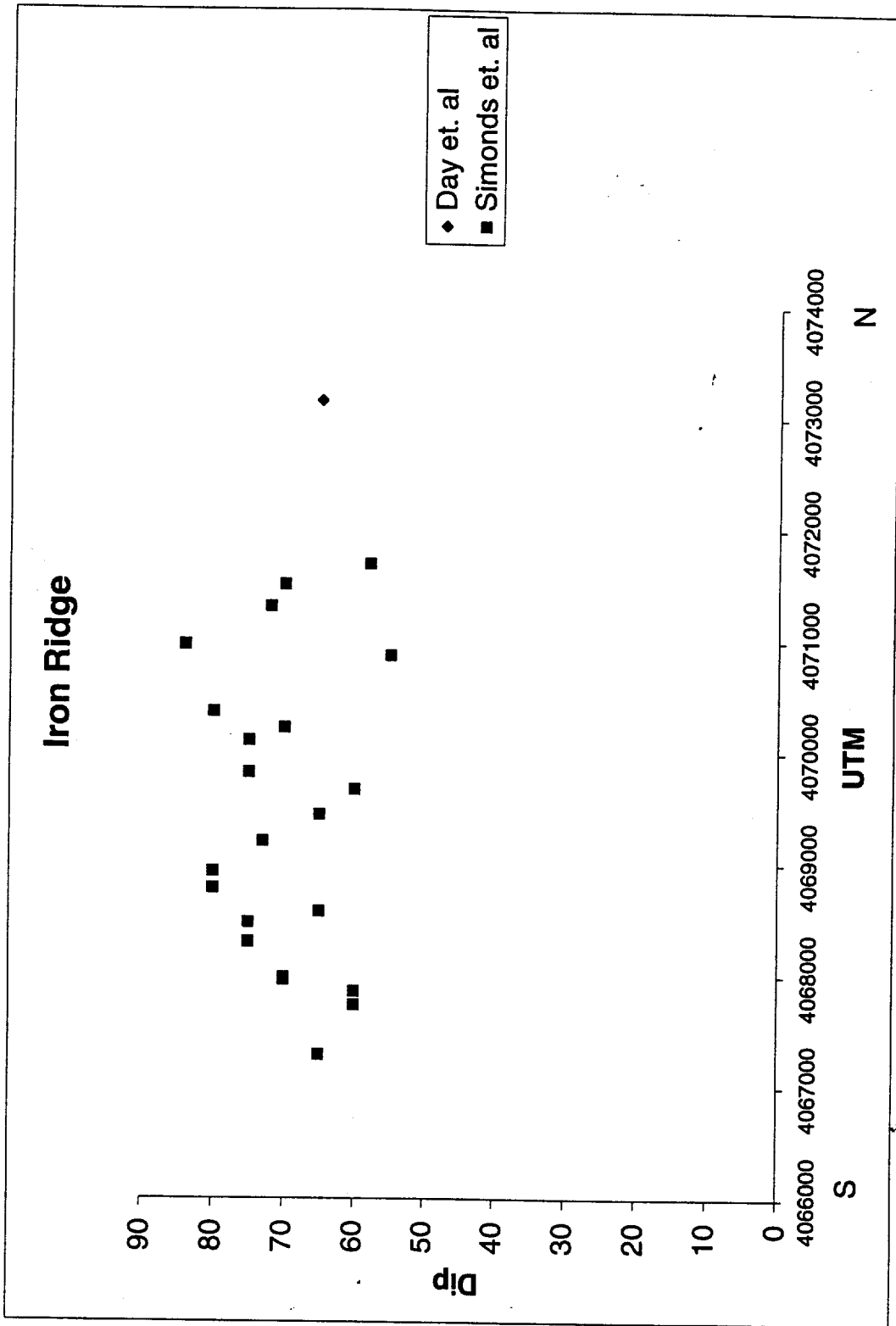


Figure 1e.

H.L. McK 7/14/00

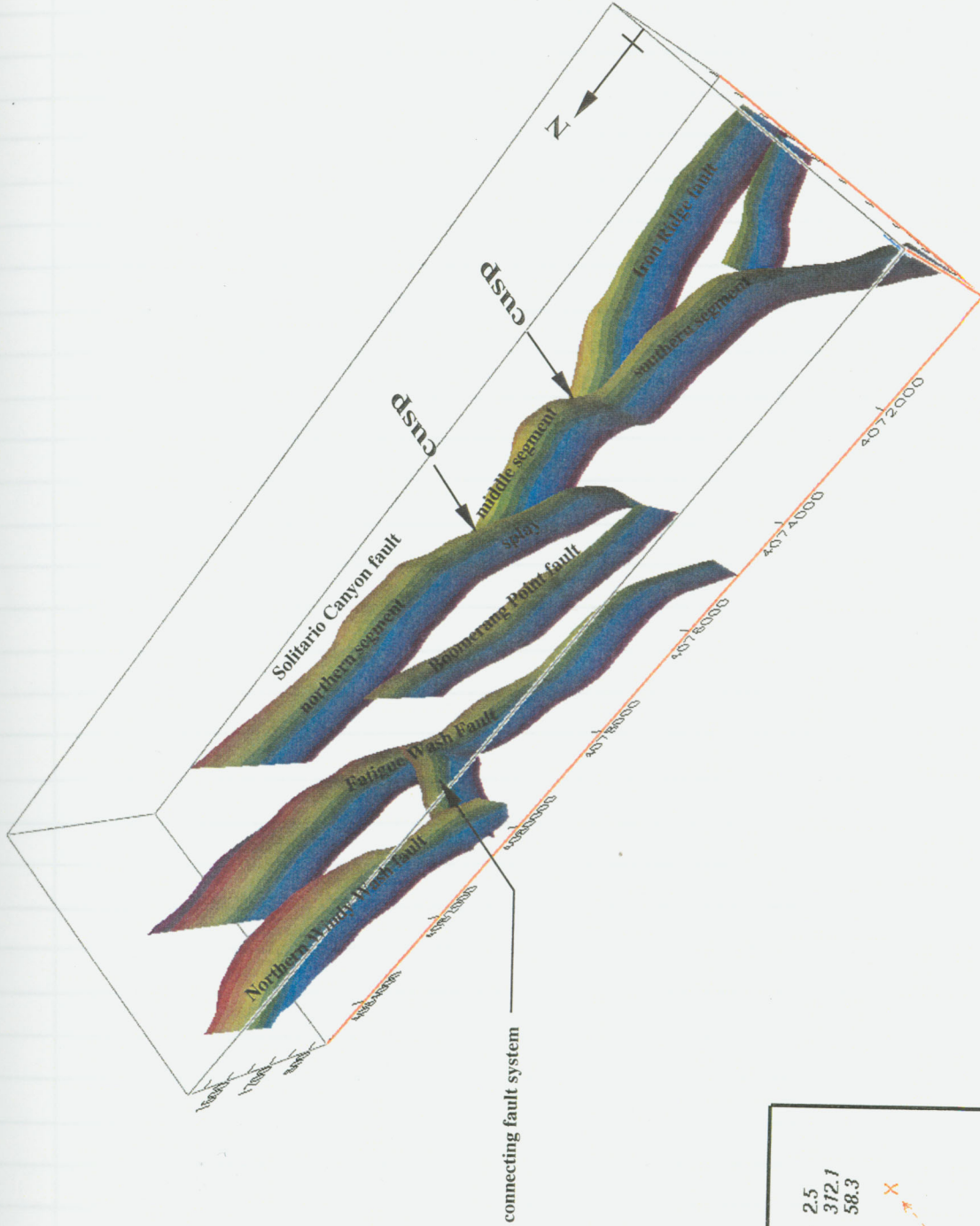


Figure 2.

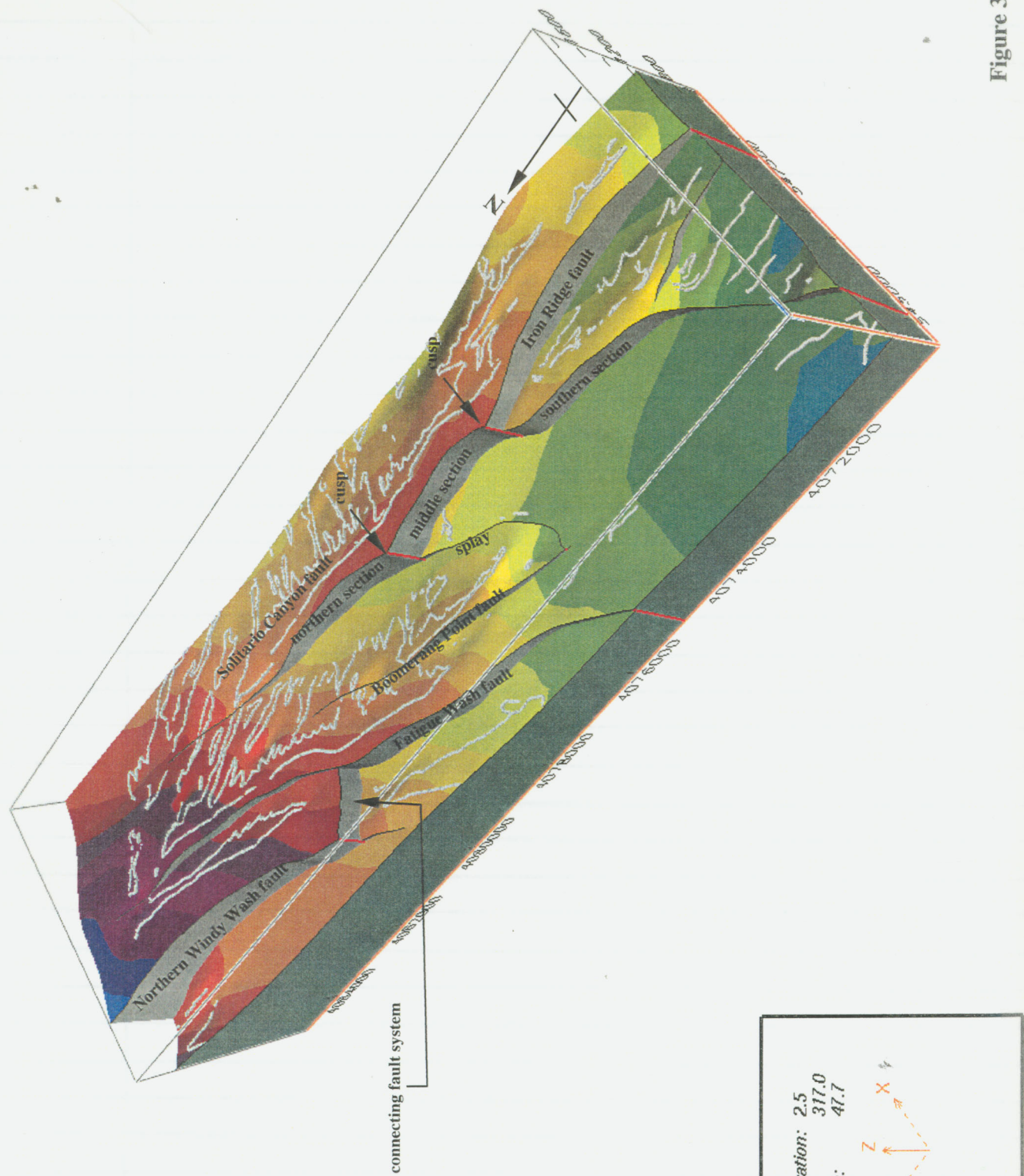


Figure 3a



Figure 3b.

Information potentially subject to copyright protection was redacted from this location. The redacted material (Figure 3b) is from the following reference:

Ferrill, D.A. J. Winterle, G. Wittmeyer, D. Sims, S. Colton, and A. Armstrong. "Fault Slip Tendency and Dilation Tendency: Implications for Anisotropic Permeability at Yucca Mountain, Nevada, Dynamics of Fluids in Fractured Rocks." Concepts and Recent Advances Meeting, Lawrence Berkeley National Laboratory. 1999.

and

Ferrill, D.A., J. Winterle, G. Wittmeyer, D. Sims, S. Colton, A. Armstrong, and A.P. Morris. "Stressed Rock Strains in Groundwater at Yucca Mountain, Nevada. GSA Today. Vol. 9, No. 5. pp. 1-8. 1999.

I have reviewed scientific notebook 247 and find it in compliance with QAP-001. There is sufficient information regarding procedure used for conducting the research and acquiring and analyzing the data so that another qualified scientist could repeat the activity or activities recorded in this scientific notebook

H. Lawrence McKague

H. Lawrence McKague
GLGP Element Manager

7/14/00

- THIS SCI NOTEBOOK
IS TO BE ARCHIVED.

*McKague
7/14/00*

